

CHAPTER VI CHANGES OF MIDGAP STATES

Since there are only a few data concerned with the peak energy location of D^0 in $a\text{-Si}_{1-x}\text{Ge}_x\text{:H}$ and there is no data concerned with that in $a\text{-Si}_{1-x}\text{C}_x\text{:H}$, a lot of researches determining their energy location should be performed by means of different techniques.

6-3. Thermal Recovery Process of Midgap-state Profile of Light-soaked Undoped $a\text{-Si:H}$

Undoped $a\text{-Si:H}$ films (about $1.2\ \mu\text{m}$ thickness) were deposited by the rf glow-discharge decomposition of pure SiH_4 . In order to measure dark conductivity (σ_2), photoconductivity ($\Delta\sigma_{ph}$), and the activation energy ($\delta_2 = E_C - E_F$) of dark conductivity in $a\text{-Si:H}$ films, samples with coplanar electrodes were fabricated by depositing $a\text{-Si:H}$ onto Corning 7059 glass substrates heated to $250\ ^\circ\text{C}$ for sample 21099 and heated to $310\ ^\circ\text{C}$ for sample AK362, and subsequently by evaporating Al at room temperature. Thus-determined properties are shown in Table 6-1. Oxygen, carbon, and nitrogen concentrations estimated using secondary-ion mass spectrometry (SIMS) were 7×10^{19} , 1×10^{19} , and $3 \times 10^{18}\ \text{cm}^{-3}$ in sample 21099, respectively, and they were 5×10^{19} , 2×10^{19} , and $8 \times 10^{17}\ \text{cm}^{-3}$ in sample AK362, respectively.

The heterojunctions were fabricated by depositing the films onto p c-Si substrates heated to $250\ ^\circ\text{C}$ for sample 21099 and heated to $310\ ^\circ\text{C}$ for sample AK362. The acceptor density (N_A) of p c-Si was $1.0 \times 10^{16}\ \text{cm}^{-3}$. Since Mg has been known to form a good Ohmic contact with undoped $a\text{-Si:H}$, Mg was then evaporated on an area ($0.785\ \text{mm}^2$) of as-deposited $a\text{-Si:H}$ films at room temperature. For other heterojunctions, Mg was evaporated after $a\text{-Si:H}$ films were exposed to the AM1 light with $100\ \text{mW/cm}^2$ at room temperature. As soon as the sample 21099 heated to $150\ ^\circ\text{C}$ in a vacuum, the transient HMC was measured using the Sanwa MI-415 capacitance meter (2 MHz). It was also measured 30-min later, 1-h later, and 2-h later. However, the transient HMC of sample AK362 could not be measured at $150\ ^\circ\text{C}$ because of low resistivity of its $a\text{-Si:H}$ film. Therefore, after the sample was

CHAPTER VI CHANGES OF MIDGAP STATES

TABLE 6-1. Film properties of samples 21099 and AK362.

Sample	As-deposited	Light exposure	Anneal ^c	Anneal ^d
21099 ^a				
σ_2 ($\times 10^{-8}$ S/cm)	0.1	0.01	0.09	0.2
$\Delta \sigma_{ph}$ ($\times 10^{-4}$ S/cm)	2	0.2	1	2
E_C-E_F (eV)	0.71	0.78	0.76	0.69
AK362 ^b				
σ_2 ($\times 10^{-8}$ S/cm)	1	0.02	0.6	2
$\Delta \sigma_{ph}$ ($\times 10^{-4}$ S/cm)	3	0.2	2	3
E_C-E_F (eV)	0.63	0.70	0.66	0.62

^a AM1, 100 mW/cm² for 3.3 h.

^b AM1, 100 mW/cm² for 4 h.

^c 150 °C for 3 h.

^d 200 °C for 1.5 h.

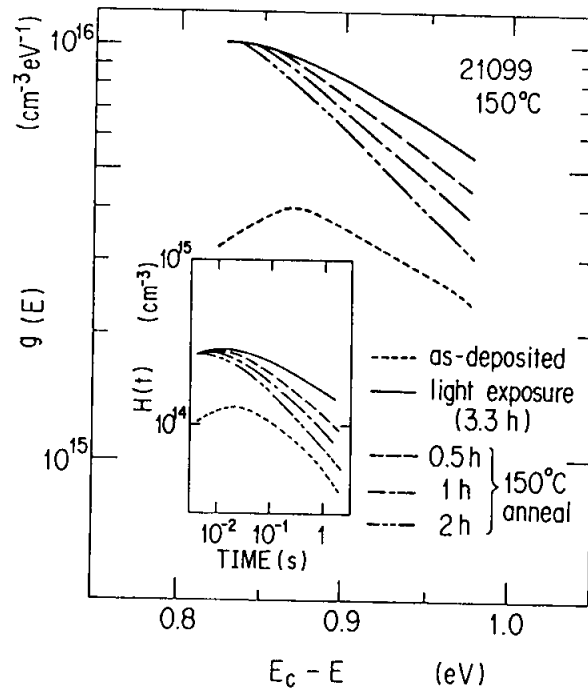


Fig.6.6. Changes of $g(E)$ at measuring temperature of 150 °C. The signal $H(t)$ of transient HMC, from which the $g(E)$ was calculated, is inserted.

CHAPTER VI CHANGES OF MIDGAP STATES

annealed at 150 °C for 3 h, the sample was cooled down, and then the transient HMC was measured at 80, 100, and 120 °C. After this, the sample was annealed at 200 °C for 1.5 h, and then the transient HMC was measured at 80, 100, 120 °C. The signal $H(t)$ of transient HMC for as-deposited films did not change before and after the heterojunctions were annealed even at 200 °C for 1.5 h in a vacuum. Figure 6.6 shows the time-resolved $g(E)$ and the corresponding signals $H(t)$ of the transient HMC in the inset. These $g(E)$ were calculated from these $H(t)$ using the attempt-to-escape frequency for electrons (ν_n) of 10^{12} s^{-1} . The signal of $H(t)$ for the as-deposited film did not change at all during the thermal annealing process at 150 °C, indicating that contact properties were not affected by this thermal treatment. Therefore, changes of $H(t)$ in the light-soaked film should be ascribed to the changes of the bulk $g(E)$ in a-Si:H.

Two sorts of models have been proposed for explaining the thermal annealing kinetics;

- (1) monomolecular kinetics,⁴⁾
- (2) bimolecular kinetics.⁵⁾

Lee et al.⁵⁾ have proposed a bimolecular annealing process with constant E_a ;

$$d[\Delta N_s(t)]/dt = -\gamma_a \exp(-E_a/kT) \Delta N_s(t)^2, \quad (6-1)$$

while Stutzmann et al.⁴⁾ have proposed a monomolecular annealing process with a distribution of E_a ;

$$d[\Delta N_s(E_a, t)]/dt = -\nu_a \exp(-E_a/kT) \Delta N_s(E_a, t). \quad (6-2)$$

Though they discussed the change (ΔN_s) of the total density estimated from ESR, the transient HMC method enables us to investigate the annealing behavior of midgap states at each energy position ($E_C - E$). Let us consider the bimolecular annealing process at each energy position;

$$d[\Delta g(E, t)]/dt = -\gamma_a \exp(-E_a/kT) \Delta g(E, t)^2 \quad (6-3)$$

and

CHAPTER VI CHANGES OF MIDGAP STATES

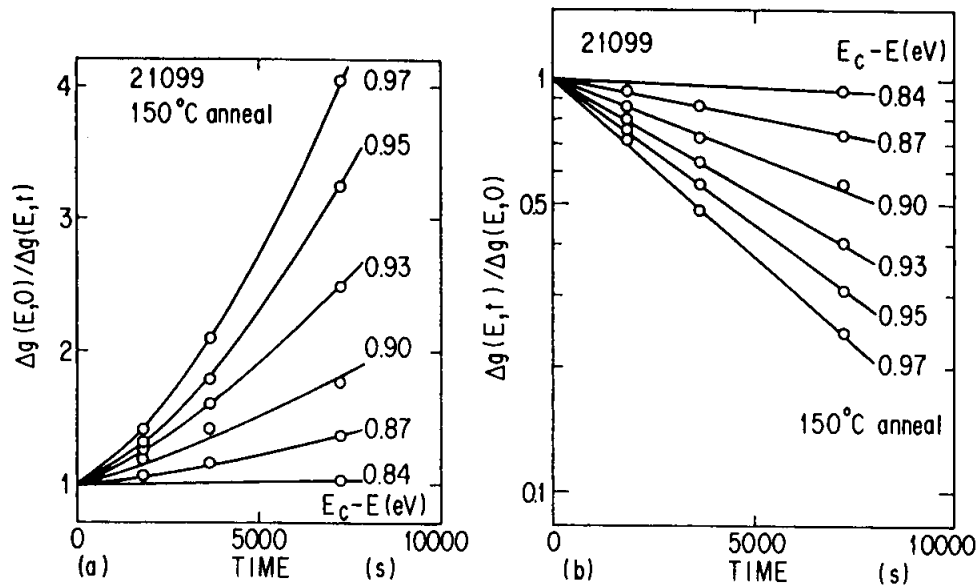


Fig.6.7. Annealing behavior of light-induced midgap states plotted assuming (a) bimolecular kinetics and (b) monomolecular kinetics.

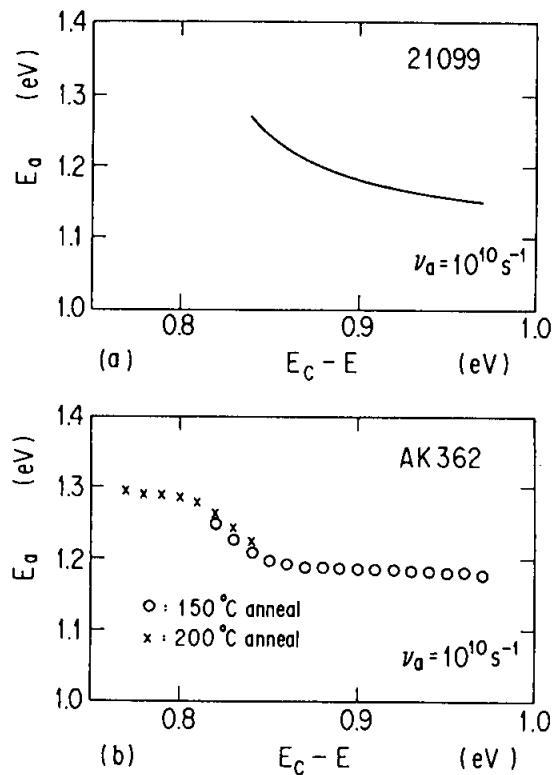


Fig.6.8. Activation energy for thermal annealing; (a) obtained from slopes in Fig.6.7(b), and (b) estimated from films annealed at 150 and 200 °C.

CHAPTER VI CHANGES OF MIDGAP STATES

$$\Delta g(E,t) = g(E,t) - g_0(E) \quad , \quad (6-4)$$

where $g(E,0)$ and $g_0(E)$ are the midgap-state profiles for the light-soaked film and the as-deposited film, respectively, t is the annealing time, and γ_a is the pre-exponential factor of the bimolecular decay rate. The integral of Eq. (6-3) implies that

$$\Delta g(E,0)/\Delta g(E,t) = 1 + \gamma_a \exp(-E_a/kT) \Delta g(E,0)t. \quad (6-5)$$

Although this equation predicts a linear relation between $\Delta g(E,0)/\Delta g(E,t)$ and t , the experimental data did not produce the straight lines, as shown in Fig. 6.7(a).

The monomolecular annealing process is given by

$$d[\Delta g(E,t)]/dt = -\nu_a \exp(-E_a/kT) \Delta g(E,t) \quad , \quad (6-6)$$

and the integral of this equation implies that

$$\ln[\Delta g(E,t)/\Delta g(E,0)] = -\nu_a \exp(-E_a/kT)t \quad , \quad (6-7)$$

where ν_a is the pre-exponential factor of the monomolecular decay rate. As is shown in Fig. 6.7(b), the data produce a straight line for each value of (E_C-E) , indicating that the experimental results can be predicted by Eq. (6-7). Values of E_a obtained from the slope of the curves of Fig. 6.7(b) are plotted as a function of (E_C-E) in Fig. 6.8(a). Here, the value of ν_a is tentatively assumed to be 10^{10} s^{-1} , which Stutzmann et al.⁴⁾ reported. The value of E_a decreases monotonously with an increase in (E_C-E) .

From the above results, at least phenomenologically, the monomolecular annealing kinetics with a distribution of E_a are more suitable for explaining these experimental data.

The behavior of E_a for states closer to the conduction band has been investigated. Although the real-time measurement of $g(E)$ in sample AK362 could not be carried out at 150 °C due to its low resistivity, E_a could roughly be estimated using Eq. (6-7) from low-temperature (80-120 °C) measurements in the films

CHAPTER VI CHANGES OF MIDGAP STATES

annealed at 150 and 200 °C. The $g(E)$ after light exposure increased by a factor of about 1.7 compared with the $g(E)$ for the as-deposited film, but the energy position of the peak of midgap states did not change by light exposure. After annealing at 150 °C for 3 h, the $g(E)$ for (E_C-E) in the range higher than 0.8 eV decreased. In the film annealed at 200 °C for 1.5 h, the $g(E)$ for (E_C-E) in the range higher than 0.85 eV approached to the $g(E)$ for the as-deposited film, while for (E_C-E) in the range lower than 0.85 eV it was still larger than the $g(E)$ for the as-deposited film. The value of E_a which was roughly estimated from this experiment is shown in Fig. 6.8(b), and E_a seems to get saturated in lower (E_C-E) .

This is the first report which elucidates the relation between E_a and (E_C-E) . Although Stutzmann et al.⁴⁾ and Smith et al.⁶⁾ predicted that midgap states should have a distribution of E_a , they did not discuss the relation between E_a and (E_C-E) . The values of E_a are similar to those reported by Qiu et al.,⁸⁾ while they are rather larger than those reported by Stutzmann et al..⁴⁾ Shepard et al.¹³⁾ have predicted from photoconductivity measurements that the $g(E)$ above the Fermi level (maybe doubly-occupied dangling bonds, D^-) closest to the midgap is annealing first, with which the present results coincide if the correlation energies between D^0 and D^- are kept constant.

6-4. Optically and Thermally Induced Reversible Changes of Midgap States in Undoped a-Si:H

Undoped a-Si:H/p c-Si heterojunctions were fabricated as follows. Undoped a-Si:H films (1.2-1.5 μm thickness) were deposited by the rf glow-discharge decomposition of pure SiH_4 gas onto p c-Si substrates heated to $T_s=200-300$ °C. After turning off the plasma, the substrate temperature was kept as it was for 10 min. Then the specimen was cooling down slowly. The acceptor density (N_A) in p c-Si was $1.0 \times 10^{16} \text{ cm}^{-3}$. Since Mg is known to form a good Ohmic contact with undoped a-Si:H, Mg was evaporated on an area (0.785 mm^2) of as-deposited films at room temperature